Keterangan tentang Pemeriksaan Similaritas menggunakan Turnitin untuk karya ilmiah berjudul:

Structure-based discovery of novel inhibitors of *Mycobacterium tuberculosis* CYP121 from Indonesian natural products

SIMILARITY INDEX 94%

Similarity dengan tulisan yang sama yang sudah beredar di internet 93%

Berarti SIMILARITY dengan karya ilmiah lain 94% - 93% = **1%**

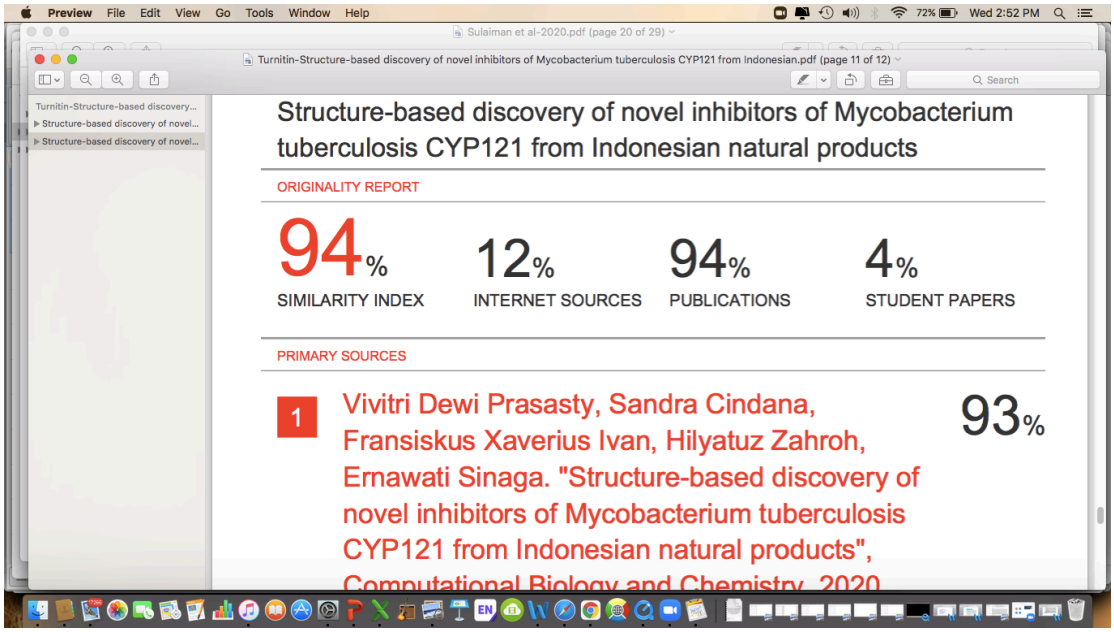

Structure-based discovery of novel inhibitors of Mycobacterium tuberculosis CYP121 from Indonesian natural products

by Ernawati Sinaga

Computational Biology and Chemistry 85 (2020) 107205

Contents lists available at ScienceDirect

Computational Biology and Chemistry

journal homepage: www.elsevier.com/locate/cbac

Structure-based discovery of novel inhibitors of *Mycobacterium tuberculosis* CYP121 from Indonesian natural products

Vivitri Dewi Prasasty[a,*], Sandra Cindana[b], Fransiskus Xaverius Ivan[b], Hilyatuz Zahroh[c], Ernawati Sinaga[d]

[a] Faculty of Biotechnology, Atma Jaya Catholic University, Jakarta, 12930, DKI Jakarta, Indonesia
[b] Department of Biotechnology, Faculty of Life Sciences, Surya University, Tangerang, 15810, Banten, Indonesia
[c] Genetics Research Centre, Universitas Yarsi, Jakarta, 10510, DKI Jakarta, Indonesia
[d] Faculty of Biology, Universitas Nasional, Jakarta, 12520, Indonesia

ARTICLE INFO

Keywords:
CYP121
Molecular docking
Molecular dynamic
Tuberculosis

ABSTRACT

Tuberculosis (TB) continues to be a serious global health threat with the emergence of multidrug-resistant tuberculosis (MDR-TB) and extremely drug-resistant tuberculosis (XDR-TB). There is an urgent need to discover new drugs to deal with the advent of drug-resistant TB variants. This study aims to find new *M. tuberculosis* CYP121 inhibitors by the screening of Indonesian natural products using the principle of structure-based drug design and discovery. In this work, eight natural compounds isolated from *Rhoeo spathacea* and *Pluchea indica* were selected based on their antimycobacterial activity. Derivatives compound were virtually designed from these natural molecules to improve the interaction of ligands with CYP121. Virtual screening of ligands was carried out using AutoDock Vina followed by 50 ns molecular dynamics simulation using YASARA to study the inhibition mechanism of the ligands. Two ligands, i.e., kaempferol (KAE) and its benzyl derivative (KAE3), are identified as the best CYP121 inhibitors based on their binding affinities and adherence to the Lipinski's rule. Results of molecular dynamics simulation indicate that KAE and KAE3 possess a unique inhibitory mechanism against CYP121 that is different from GGJ (control ligand). The control ligand alters the overall dynamics of the receptor, which is indicated by changes in residue flexibility away from CYP121 binding site. Meanwhile, the dynamic changes caused by the binding of KAE and KAE3 are isolated around the binding site of CYP121. These ligands can be developed for further potential biological activities.

1. Introduction

Tuberculosis (TB) is an infectious disease caused by *Mycobacterium tuberculosis*. It is estimated that about 1,500,000 people worldwide have died from TB and 9.8 million people have been infected by TB (WHO, 2015). The disease has spread worldwide with a varying number of cases in each country, where Indonesia ranks second after India as the country with the most TB cases (CDC, 2015). Jakarta became the city with the lowest prevalence with 29 cases, while Papua had the highest prevalence with 2,738 cases. The geographical challenges in Indonesia cause the unavailability of adequate health facilities in certain regions. Surveys on 482 districts in Indonesia, only 71 % of districts are served by the government health officers (Collins et al., 2013).

M. tuberculosis commonly affects the lungs with symptoms of persistent cough, coughing up blood (hemoptysis), fever, loss of appetite, weight loss, and hyperhidrosis in humans (CDC, 2015). *M. tuberculosis* can spread from TB patients to healthy person around them through the air. When people with TB cough or sneeze, TB bacteria will come out in the form of splashes (droplets) and stay in the air for several hours until they find a new host (Saleem and Azher, 2013). A TB patient can cause 10–15 other healthy people to become infected with TB if the patient is in direct contact with them for a year (Kanabus, 2016).

To deal with the increasing cases of tuberculosis, the Indonesian Ministry of Health has issued guidelines for the management of tuberculosis based on the Directly Observed Treatment Short-Course Therapy (DOTS) strategy since 1995. TB treatment standard based on the DOTS strategy is to use a mixture of two bactericidal drugs for 6 months. Patients who follow this treatment program should be closely monitored by a doctor and required to complete the treatment (Ministry of Health RI, 2011). Due to the length of treatment and the lack of discipline and supervision, many patients do not complete the treatment program. It causes the infection cannot be eliminated thereby

* Corresponding author.
E-mail address: vivitri.dewi@atmajaya.ac.id (V.D. Prasasty).

https://doi.org/10.1016/j.compbiolchem.2020.107205
Received 23 December 2019; Accepted 14 January 2020
Available online 17 January 2020
1476-9271/

triggering the emergence of new TB bacteria that are resistant to commonly used bactericidal drugs (Kanabus, 2016).

Today the world is facing a global crisis caused by the emergence of new multidrug-resistant (MDR) and extensively drug-resistant (XDR) TB bacteria. Bacteria resistant to these standard TB drugs still belong to the same species (*M. tuberculosis*), but these bacteria can adapt by changing their cell structure so that standard bactericidal drugs for TB become ineffective (Nzila et al., 2011). The Indonesia government has monitored the cases of MDR-TB since 2010 and it is expected to become more serious if there is no effort to find new types of drugs capable of fighting the MDR-TB and XDR-TB (Ministry of Health RI, 2011).

Efforts to discover new antituberculosis drugs can be done through a variety of strategies, one of which is the use of medicinal plants. Indonesia is the host of about 7,000 species of medicinal plants that have been used for generations to treat various types of diseases (Bermawie, 2004), and some medicinal plants containing antituberculosis active compounds have been identified (Ramyanti et al., 2013; Mohamad et al., 2011; Chinsembu, 2016; Saludes et al., 2002). Some medicinal plants reported having good antituberculosis activities are *Rhoeo spathacea* and *Pluchea indica*. The leaf extract of these two plant species potentially inhibits the growth of *M. tuberculosis* of the native strain and the MDR strain of TB (Radji et al., 2015a).

Another strategy for finding antituberculosis drugs is to look for new drug targets. The current targets of commercial antituberculosis drugs are DNA gyrase, which is the target of the fluoroquinolone, the biosynthesis of mycolic acid which is the target of the isoniazid, and RNA polymerase which is the target of rifampicin (Barry et al., 2006). One of the most potential target molecules for a new antituberculosis drug is the CYP121 enzyme that is one of the members of the P450 cytochrome enzyme group in *M. tuberculosis*. This enzyme plays a vital role in the oxidation process of several compounds, such as steroids, fatty acids, and xenobiotics (Leys et al., 2002). CYP121 is an essential enzyme for the viability of *M. tuberculosis*; therefore, this enzyme can be a promising new drug target (McLean et al., 2008).

The modern drug discovery and development practices employ computers to find new drug candidates with specific biological activity. This method, called Computer-Aided Drug Design (CADD), utilizes data in the form of a three-dimensional structure of various biomolecular receptors as targets for drug candidates. The CADD method has now been developed into a more sophisticated technique called Virtual High Throughput Screening (vHTS) that can screen millions of molecules as potential drug candidates in a relatively short time (Sliwoski et al., 2014).

This study was carried out to respond to the severe threat of MDR-TB and XDR-TB by finding active compounds isolated from *Rhoeo spathacea* and *Pluchea indica* that act as inhibitors of *M. tuberculosis* CYP121 through structure-based virtual screening. Sixteen natural compounds and their derivatives were virtually screened using molecular docking to find the most potent inhibitors. We discovered that kaempferol (KAE) and its benzyl-derivative (KAE3) are the best CYP121 inhibitors. Further investigation using molecular dynamics simulation shows that both molecules inhibit the CYP121 by affecting the dynamics of the CYP121 binding pocket. These compounds can be further tested to confirm their biological activities against TB.

2. Materials and methods

2.1. Materials

PyMol (DeLano Scientific LLC, USA) and DS Visualizer (Accelrys, Inc., USA) were employed to visualize and modify the receptor and ligand structures. A molecular format conversion program, OpenBabel (O'Boyle et al., 2011) was used to convert various ligand formats. Pre-docking molecular topology preparation was done using SwissParam (http://www.swissparam.ch/) (Zoete et al., 2011). AutoDock Vina (Trott and Olson, 2010) was the primary docking program used in this work. The preparation of the *M. tuberculosis* CYP121. pdbqt file and determination of the grid box size were carried out using AutoDock Tools (The Scripps Research Institute, La Jolla, USA). Analysis of post-docking results was carried out using LigPlot (Anon, 2020; Laskowski and Swindells, 2011; Wallace et al., 1996). Molecular dynamics (MD) simulations were performed using YASARA Structure (Krieger et al., 2002). Lipinski's rule evaluation on ligands was performed using Sanjeevini (http://www.scfbio-iitd.res.in/sanjeevini/sanjeevini.jsp) (Jayaram et al., 2012a).

2.2. Methods

2.2.1. Preparation of CYP121 structure for molecular docking

The three-dimensional structure of CYP121 in complex with inhibitor fragment 24a was retrieved from Protein Data Bank (PDB ID: 5IBD). The CYP121 structure was prepared for molecular docking processes by removing all sulfate ions and water molecules. Ligand (GGJ) was removed and saved as a separate. pdb file for validation docking.

2.2.2. Ligand preparation for molecular docking

The three-dimensional structures of the natural product ligands were retrieved from PubChem in. sdf format (Kim et al., 2016). The compounds used in this work were rutin PubChem CID: 5280805, epigallocatechin gallate PubChem CID: 65064, peltatoside PubChem CID: 5484066, chlorogenic acid PubChem CID: 1794427, caffeic acid PubChem CID: 689043, quercetin PubChem CID: 5280343, kaempferol PubChem CID: 5280863, and myricetin PubChem CID: 5281672. The derivatization of natural ligands was carried out in two steps: i) the best docked conformation of natural product ligand was visually observed, and a functional group was added to the ligand using the Avogadro program (Hanwell et al., 2012) to maximize the interactions between ligand and CYP121, and ii) the derivatized ligands were docked to CYP121 and only ligands with better binding affinities than their parent ligands were taken for further investigation. The derivatized ligands were initially prepared by substituting side chain groups of 8 parent ligands with methyl, amine, benzene, toluene and dinitro-benzenamine to obtain 40 derivative ligands.

2.2.3. Molecular docking

Molecular docking was carried out using AutoDock Vina (Trott and Olson, 2010) version 1.1.2, which runs under Microsoft Windows 7 operating system. AutoDock Vina was used based on its accuracy and speed, which is higher than its predecessor software, AutoDock 4. AutoDock Tool was utilized to prepare the input.pdbqt file for CYP121 and to set the size and the center of the grid box. Kollman charges and polar hydrogen atoms were added to the CYP121 structure. The center of the grid box was set at -8.728, 18.327, and 3.430 in the dimensions of x, y and z, respectively using 1.000 Å spacing and box size of 30 × 30 × 30. Validation of the docking parameters was done by re-docking the co-crystalized ligand into the active site of the CYP121 receptor. Analysis of post-docking results was carried out using LigPlot+ (Laskowski and Swindells, 2011; Wallace et al., 1996).

2.2.4. Molecular dynamics

Molecular dynamics (MD) simulations were performed using YASARA Structure (Krieger et al., 2002) version 14.12.2, and run under Microsoft Windows 8.1 operating system. The force field used in this simulation was the AMBER03 force field. Long-distance Coulomb interactions were calculated using the Ewald particle algorithm, while the Van der Waals force was limited to 8 Å. A cube-shaped simulation box was placed around a simulated molecule with a distance of 5 nm. The simulated box size was 50 × 50 × 50 Å with the value of n = 6. The boundary of the simulated box was conditioned in the periodic form. The water density was set at 1 g / cc at the temperature of 298 K. The simulation was run for 50 ns with snapshots taken every 100 ps. Visualization and analysis were carried out using macro files

implemented in YASARA Structure. Two primary analyses were performed on the MD trajectories, i.e., root mean square deviation (RMSD) using *md_analyze.mcr* macro and root mean square fluctuation (RMSF) for each residue using *md_analyzeres.mcr* macro.

2.2.5. Drug-likeness properties

Determination drug-likeness properties for ligands were done by following Lipinski's rules to ensure whether all ligand meet the requirements to be used as drug molecules. These drug-likeness properties are done by using the Sanjeevini program (Jayaram et al., 2012b), which can be accessed through the website address http://www.scfbio-iitd.res.in/software/drugdesign/lipinski.jsp#anchortag. Data that must be entered on this site must be in. mol2 format.

3. Results and discussion

In this work, we virtually screened potential inhibitors against *M. tuberculosis* CYP121. Ligands used in this study are compounds isolated from Indonesian herbs, namely *Rhoeo spathacea* and *Pluchea indica*. The natural compounds isolated from *Rhoeo spathacea* are epigallocatechin (EPI), rutin (RUT), and peltatoside (PEL) (Tan et al., 2015), while the active compounds isolated from *Pluchea indica* are chlorogenic acid (CHL), caffeic acid (CAF), quercetin (QUE), kaempferol (KAE), and myricetin (MYR) (Suriyaphan, 2014).

The derivatives of each natural compound were prepared by adding various functional groups to the best docked conformation of each molecule. The new functional groups were aimed to improve the interaction between ligand and the protein receptor by filling up the "unoccupied pocket" on the binding site by an appropriate functional group. The choice of functional groups to be added to the parent ligands was made according to the properties of the receptor's amino acid residues around the natural ligand. All derivatized ligands were docked into CYP121 and only the ligands with better binding affinity to the protein receptor were taken for further investigation.

Lipinski's rule validation was carried out to evaluate whether every ligand meets the requirements as an orally active drug molecule, i.e., has the molecular weight of about 500 g/mol, has less than five hydrogen bond donors, has less than ten hydrogen bond acceptors, and has the logP value of less than 5 (Lipinski et al., 1997) as shown in Table 1. Four natural ligands violate Lipinski rules, i.e., RUT, EPI, PEL, and MYR, whereas five derivatized ligands violate Lipinski rules, i.e., RUT12, EPI7, PEL1, CHL8, and MYR3. There are eight ligands that follow Lipinski's rule, i.e. GGJ (control, 4-(3′-amino[1,1′-biphenyl]-3-yl)-3-(4-methoxyphenyl)-1H-pyrazole-5-amine), CHL, CAF, CAF5, QUE, QUE3, KAE, and KAE3. Among those ligands that meet the Lipinski's rule, KAE and KAE3 are ligands with the strongest interaction with

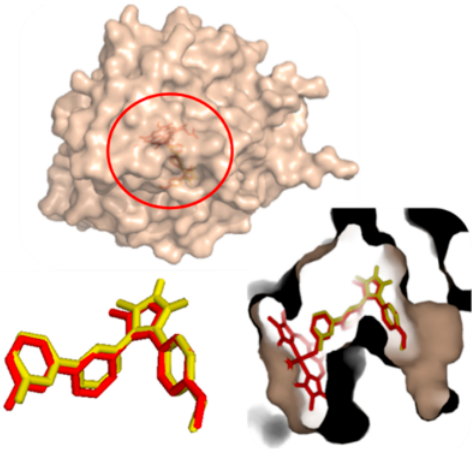

Fig. 1. Redocking of GGJ into CYP121 binding pocket. The crystallized conformation of GGJ is shown in the red stick structure. The best-redocked pose of GGJ is shown in yellow stick structure using Pymol. The position of GGJ in the binding pocket of CYP121 is indicated in the red circle.

CYP121 as indicated by their binding affinities, i.e., -9.1 kcal/mol and -10.5 kcal/mol, respectively. Therefore, KAE and KAE3, together with GGJ were further investigated using molecular dynamics simulation.

3.1. Molecular docking

Docking validation was carried out to ensure that ligands bind to the binding pocket in the correct conformation. In this study, docking validation was performed by re-docking the GGJ ligand into the CYP121 receptor. We found that the binding conformation of redocked GGJ reproduced the binding mode of the co-crystallized ligand with the binding affinity of -11.5 kcal/mol. Fig. 1 shows the docking validation results with the original red ligand and the yellow docking validation ligand. Both structures were superimposed to show that the size and coordinate center parameters used in the molecular docking were able to reproduce the crystalized conformation of GGJ.

We performed molecular docking on 48 molecules consist of natural and derivatized ligands. These molecules were ranked based on their binding affinities. Table 2 lists the 16 compounds that consist of eight natural product compounds and eight derivatized ligands. The rational basis of selecting the eight derivatized ligands is that only derivatized

Table 1
The results of the selection of Lipinski rules for 17 ligands.

No.	Constituent	Code	Molecular weight (g/mol)	Hydrogen bond donor	Hydrogen bond acceptor	LogP	Violation of Lipinski's rule
1	Control	GGJ	356	5	4	4.58	0
2	Rutin	RUT	610	10	16	−1.88	3
3	Myricetin	MYR	318	6	8	1.72	1
4	Peltatoside	PEL	606	11	16	−4.32	3
5	Kaempferol	KAE	286	4	6	2.31	0
6	Quercetin	QUE	302	5	7	2.01	0
7	Chlorogenic acid	CHL	353	5	9	−1.98	0
8	Epigallocatechin	EPI	306	6	7	1.25	1
9	Caffeic acid	CAF	179	2	4	−0.14	0
10	Rutin12	RUT12	623	11	16	−1.69	3
11	Myricetin3	MYR3	425	9	10	2.40	1
12	Kaempferol3	KAE3	346	3	5	4.27	0
13	Epigallocatechin7	EPI7	398	7	8	2.62	1
14	Peltatoside1	PEL1	620	11	16	−4.01	3
15	Chlorogenic acid8	CHL8	434	8	11	−2.28	2
16	Quercetin3	QUE3	378	5	7	3.67	0
17	Caffeic acid5	CAF5	269	2	4	1.84	0

Table 2
List of 16 natural and derivatized ligands used in this study with their binding affinities.

Natural/parent ligand	Binding affinity (kcal/mol)	Derivatized ligand	Binding affinity (kcal/mol)	The functional group(s) added to the parent ligand
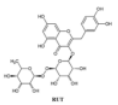	−10.6	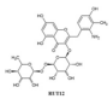	−11.0	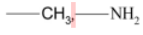
	−8.2		−10.4	
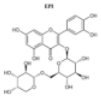	−9.3	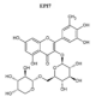	−10.3	
	−9.3	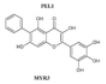	−10.6	
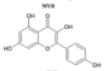	−9.1	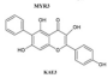	−10.5	
	−8.9		−10.0	
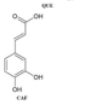	−7.2	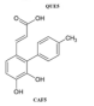	−8.5	
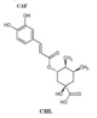	−8.8	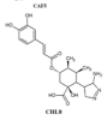	−10.1	

compounds with binding affinities higher than that of their parent natural compounds are included in the list for further investigation.

Ligand GGJ is stabilized by interacting with 13 amino acid residues through hydrophobic interactions, i.e., Thr77, Val78, Val82, Val83, Ala167, Phe168, Val228, Thr229, Gly232, Ala233, Ser237, Phe280, and Arg386. GGJ is also stabilized by three hydrogen bonds between its N25 nitrogen atoms with OG oxygen atom of Ser237 and two nitrogen atoms at the center of the HEM group (Fig. 2).

Ligand KAE is stabilized by 13 hydrophobic contacts with Val78, Val82, Ser163, Leu164, Ala167, Phe168, Ala178, Asn181, Trp182, Asp185, Val228, Thr229, and Gly232, where seven of them are similar to the hydrophobic contacts that stabilize GGJ, which indicates that KAE and GGJ have similar pattern of interactions. KAE is also stabilized by five hydrogen bonds between its O3 oxygen atom with O atom of Ala178 and N atom of Trp182, O4 oxygen atom with the OD2 oxygen atom of Asp185, O5 oxygen atom with the O22 oxygen atom of Val228, and N atom of Ala233. Interestingly, KAE3 has different residual contacts with its parent ligand, KAE. KAE3 is stabilized by hydrophobic contacts with Met62, Thr65, Val78, Val82, Val83, Ala167, Phe168, Trp182, Val228, Thr229, Gly232, and Pro285. KAE3 is also stabilized by four hydrogen bonds between its O5 oxygen atom with the OG1 oxygen atom of Thr65 and O oxygen atom of Pro285, and O2 oxygen atom with O oxygen atom of Thr77 and OG1 atom of Ala167 (Fig. 3).

3.2. Molecular dynamics

In this study, molecular dynamics simulation was performed to study the effect of ligand binding on the molecular dynamics of the receptor. In contrast to the molecular docking, molecular dynamics can simulate receptors and ligands flexibility and allows the receptors to move and adjust the conformation with binding ligands (Alonso et al., 2006). In molecular dynamics, complex molecules are simulated in the (cell) system filled by a particular solvent so that the complex conformation can change.

In this study, the molecular dynamics simulation was performed using YASARA Structure (Krieger et al., 2002). Molecules simulated in molecular dynamics are CYP121 without ligand (code: RES), CYP121 complexed with GGJ ligand (code: GGJ), CYP121 complexed with KAE ligand (code: KAE), and CYP121 complexed with KAE3 ligand (code: KAE3). Ligands KAE and KAE3 are the best binders to CYP121 among ligands that meet the requirements of Lipinski's rule.

Molecular dynamics simulates the conformational change of a molecular system by modeling the movement of all atoms in the system in a three-dimensional space. This conformation change can be analyzed by looking at the simulated time curve of RMSD (root mean square deviation), with RMSD value as the amount of conformational change experienced by a molecular system relative to the initial conformation at $t = 0$.

Root mean square deviation (RMSD) analyses of all four simulations show that the conformations of CYP121 reach a plateau in 10 ns. The RMSD values of the RES system are more fluctuative than that of the other systems. The RMSD curve shows to be stable up to 13 ns with an average RMSD value of 1.17 Å, which indicates that the molecular conformation of the RES system does not change significantly at this period (Fig. 4). However, the RMSD curve starts to fluctuate after 13 ns up to 48 ns. It suggests that the protein adopts several different conformations within that period. Furthermore, the RMSD curve starts to stabilize back up to 50 ns. The fluctuation of the RES system could be due to the absence of the ligand in the binding pocket of the receptor

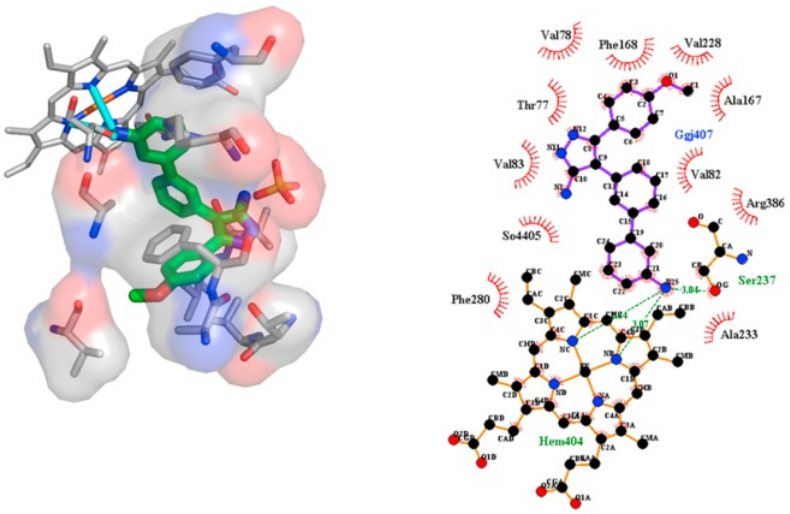

Fig. 2. Binding conformation of GGJ inside CYP121 binding pocket. (a) Ligand GGJ is shown in green carbons using Pymol. (b) Two-dimensional plot of interactions between GGJ and surrounding residues using Ligplot. Hydrogen bonds are indicated in green dashed line. Residues with hydrophobic contacts with the ligands are indicated in the eyelash symbol.

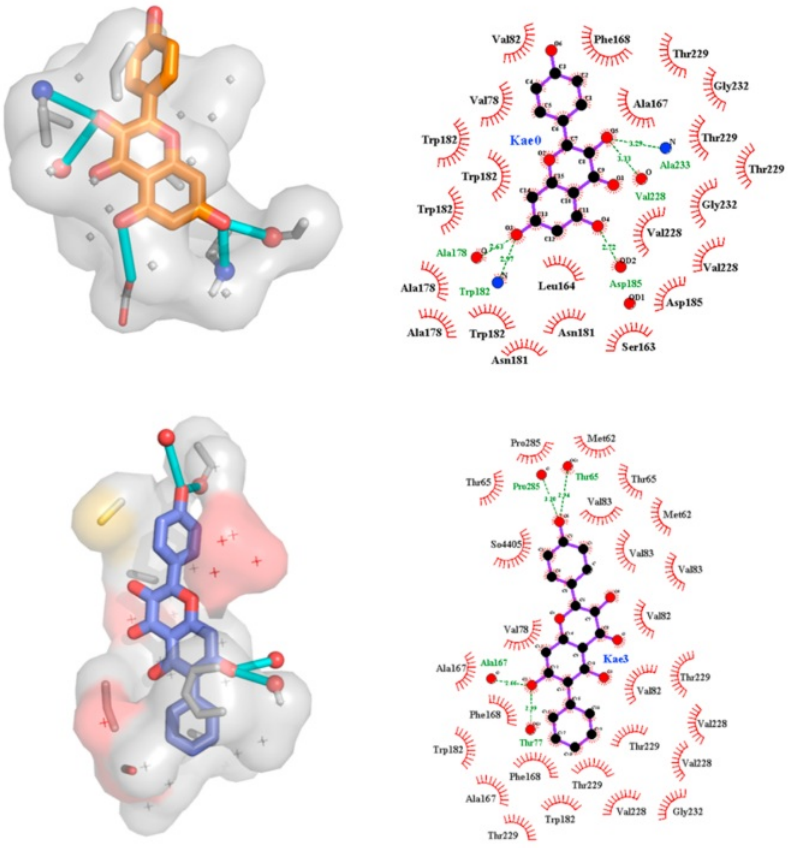

Fig. 3. Binding conformation of KAE (upper panel) and KAE3 (lower panel) inside CYP121 binding pocket. (a) Ligand KAE is shown in orange carbons. (b) Two-dimensional plot of interactions between KAE and surrounding residues. Hydrogen bonds are indicated in green dashed line. Residues with hydrophobic contacts with the ligands are indicated in the eyelash symbol. (c) Ligand KAE3 is shown in blue carbons. (b) Two-dimensional plot of interactions between KAE3 and surrounding residues. Hydrogen bonds are indicated in green dashed line. Residues with hydrophobic contacts with the ligands are indicated in the eyelash symbol. (a) & (c) are visualized using Pymol; (b) & (d) are visualized using Ligplot.

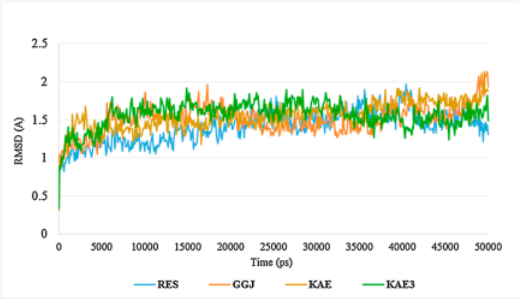

Fig. 4. Root mean square deviation (RMSD) plot of four systems (RES, GGJ, KAE, KAE3) over 50 ns MD simulation.

that causes the protein to explore more conformational space.

In the GGJ system, the RMSD values reached a plateau within 6 ns and remained stable 48 ns before looking for a new conformation after 49 ns. Conformational changes experienced by the GGJ system are fewer compared to the RES system indicating that the presence of ligand in the binding pocket of CYP121 limits the flexibility of the receptor to explore more conformational space. The natural ligand KAE and derivatized ligand KAE3 systems show similar characters as the GGJ system, where the stabilization of protein conformation is obtained within 6 ns.

Ligand binding can stabilize a protein receptor by creating molecular interactions with amino acid residues on the binding pocket; thus, restricting the flexibility and dynamics of the receptor. The ability of a ligand to improve a receptor's stability, or melting temperature (Tm), is the most predictive measure to identify promising candidate ligands for crystallization trials, with 92% of crystallized ligand-receptor pairs possessing a Tm above 55 °C (Alexandrov et al., 2008; Zhang et al., 2015). Miller et al. (2015) conducted a brute force approach for identifying ligands that stabilize receptors using G protein-coupled receptors (GPCRs). They concluded that ligand with higher potency to bind to GPCRs is correlated with ligand's ability to induce receptor stability (Miller et al., 2015).

Molecular dynamics simulation allows the movement of amino acid residues on the protein. The value of this movement over a particular time range can be analyzed by calculating the RMSF (root mean square fluctuation) value. The fluctuations of amino acid residues and overall molecular dynamics of the receptor may be affected by the presence of ligands that interact with amino acid residues on and around the binding pocket (Skjaerven et al., 2011).

First, we compared the RMSF values between the RES and GGJ systems (Fig. 5a). There are 77 amino acid residues in the GGJ system whose RMSF value changed by more than 50 % compared to the RMSF values in the RES system, which suggests that the presence of GGJ ligand causes a change in the fluctuation of 77 amino acid residues. From 77 amino acid residues, two residues have hydrophobic interaction with GGJ ligand, i.e., Gly232 and Ala233, which are located in the binding pocket of CYP121 (Fig. 5b). The change in RMSF values was seen most significantly on Pro104 residue with an increase of 300 % compared to its value in the RES system. It is quite interesting because Pro104 does not interact directly with the ligand. The high value of RMSF on Pro104 suggests that the presence of GGJ ligand in receptor molecules does affect not only the flexibility of amino acid residues around the binding site but also affects the flexibility of amino acid residues that do not interact directly with the GGJ ligand. Fig. 7b shows the location of 77 amino acid residues in receptor molecules undergoing RMSF changes in the presence of GGJ ligand.

Fig. 6a shows the comparison between RMSF values of the RES and KAE systems. There are only seven amino acid residues which RMSF values changed by more than 50 % in the presence of KAE ligand, i.e.,

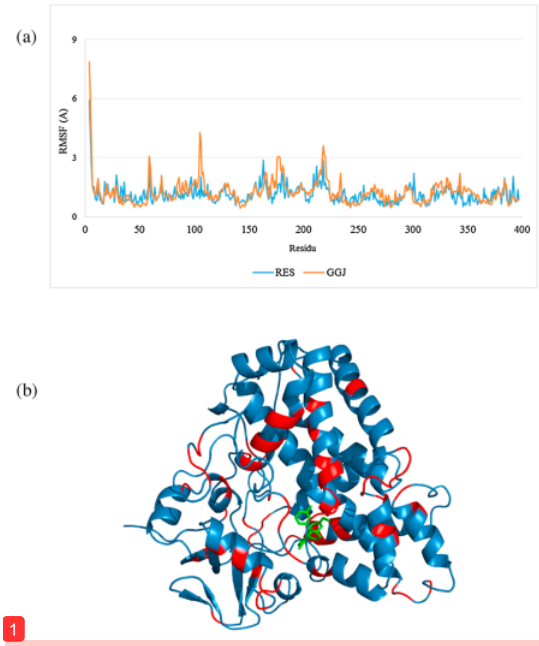

Fig. 5. The flexibility of amino acid residues on RES and GGJ systems. (a) Root mean square fluctuation (RMSF) of each amino acid residue on RES (blue) and GGJ (red) systems. (b) Positions of amino acid residues in the GGJ system whose RMSF value changed by more than 50 % compared to the RMSF values in the RES system are indicated in red.

Arg26, Thr77, Pro79, Asn118, Ser170, Ile175, and Ala178. From seven amino acids, only Ala178 residue has direct interaction with KAE ligand (Fig. 6b). Although there is only one residue that interacts directly with KAE ligand, five residues that have an RMSF value increase of more than 50 % are located in the ligand binding site. There are only two residues that do not lie in the binding site, i.e., Arg26 and Asn118. Despite being distant from the binding site and does not interact directly with the KAE ligand, these two residues have a rather high RMSF value increase when compared to the residues located on the binding site.

Fig. 7 a shows the comparison between RMSF values of the RES and KAE3 systems. There are only eight amino acid residues with RMSF values changed by more than 50 %, i.e. Arg14, Val82, Ser170, Glu221, Phe231, Asp282, Pro332, and Leu392. From eight residues, only Val82 has direct interaction with the KAE3 ligand (Fig. 7b). Three of the eight amino acid residues (Arg14, Pro332, and Leu392) are distant from the receptor binding site, whereas the other five amino acid residues are located on the binding site.

In general, the effect of the GGJ ligand on the dynamics of the amino acid residue is more prominent than that of KAE and KAE3 ligands. However, most of the amino acid residues affected by the GGJ ligand are located far from the active site of the receptor. From 77 amino acid residues whose RMSF values affected by the presence of the GGJ ligand, there are only two residues interact directly with the ligand. In contrast, the presence of KAE ligand only causes seven amino acid residues to change the value of RMSF with five amino acid residues among them located on the binding site of the receptor molecule, while on KAE3 ligand, eight amino acid residues are undergoing dynamic changes as a result of the presence of KAE3 ligands. Five of the eight residues of which are located on the binding site of the receptor molecule.

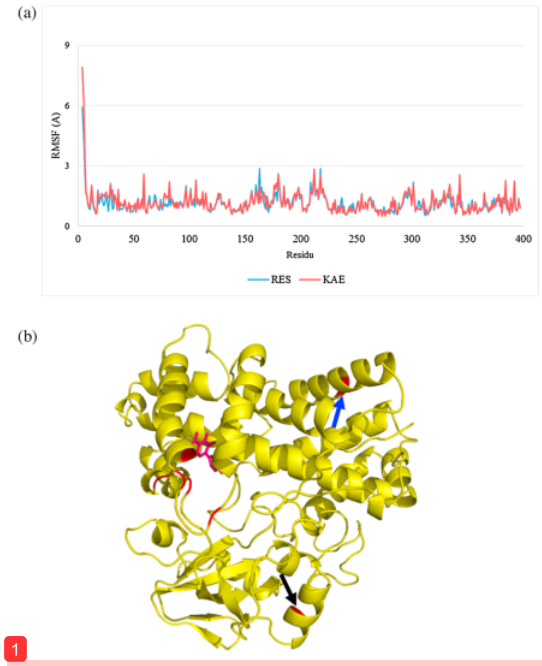

Fig. 6. The flexibility of amino acid residues on RES and KAE systems. (a) Root mean square fluctuation (RMSF) of each amino acid residue on RES (blue) and KAE (red) systems. (b) Positions of amino acid residues in the KAE system whose RMSF value changed by more than 50 % compared to the RMSF values in the RES system are indicated in red.

By comparing the RMSF values of the four systems (RES, GGJ, KAE, and KAE3), it suggests that GGJ causes a change in the conformation of amino acid residues both on the binding site and distant amino acid residues, whereas KAE and KAE3 only cause changes in amino acid residue on the binding site. The inhibitory mechanism performed by GGJ ligand is thought to affect changes in the conformation of the whole amino acid residues while the inhibitory mechanisms of KAE and KAE3 ligands alter the conformation of the amino acid residue on the binding site.

The change of the dynamics of amino acid residues located away from the ligand and the binding site is known as long-range effect phenomenon caused by the "domino effect", i.e. the change in one amino acid residue is transmitted to the adjacent residue and then forwarded to the next residue. Oelschlaeger and colleagues first modeled the domino effect on the enzyme by studying metallo-β-lactamases (Oelschlaeger et al., 2003). In their study, the impact of the mutation on Gly196 on the dynamics of metallo-β-lactamases IMP-1 and IMP-6 was investigated using molecular dynamics simulation. The amino acid only distinguishes IMP-1 and IMP-6 on position 196, which is located far from the active site of the enzyme, i.e. Gly196 for IMP-6 and Ser196 for IMP-1. This mutation can cause changes in the specificity of metallo-β-lactamases to cephalosporin. The following mechanism explains the effect of the mutation on residue 196: when Gly replaces ser, a hole exists which causes the loss of interaction between Ser196 and Lys33. The loss of interaction between the two amino acid residues causes increased flexibility in the surrounding residues, and this effect is then transmitted to the binding site of metallo-β-lactamase.

The long-range effect plays an important role in the allosteric mechanism of the enzyme inhibition, specifically when the ligand binds to the enzyme not on its active site but is capable of affecting the activity of the enzyme. Conformational changes and dynamics on the allosteric

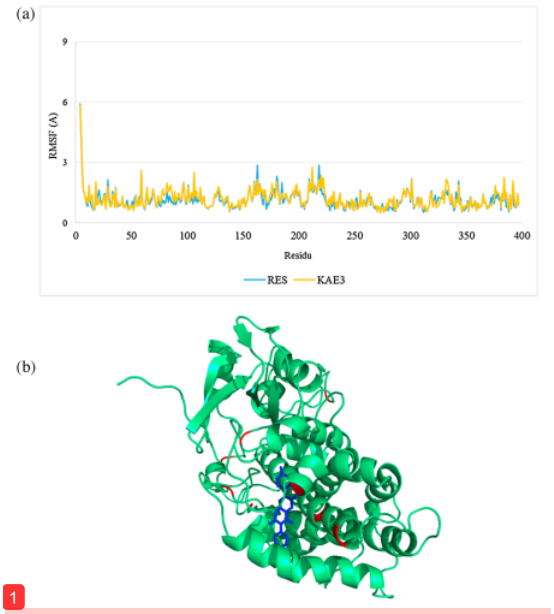

Fig. 7. The flexibility of amino acid residues on RES and KAE3 systems. (a) Root mean square fluctuation (RMSF) of each amino acid residue on RES (blue) and KAE3 (orange) systems. (b) Positions of amino acid residues in the KAE3 system whose RMSF value changed by more than 50 % compared to the RMSF values in the RES system are indicated in red.

site are transmitted to other distant amino acid residues, which influence the conformation and the dynamics of the protein as a whole. Vettoretti and coworkers conducted a detailed study of the mechanism of allosteric activation by different types of ligands against Hsp90 using molecular dynamics simulation (Vettoretti et al., 2016). In their study, the long-range effect is explained by a different mechanism than that proposed by Oelschlaeger et al. (2003). Vettoretti et al. proposed the receptor conformation selection mechanism for attachment with ligands. After the attachment of the ligand occurs, the population shifts towards a conformation chosen by the ligand. The theory of conformational population selection is also proposed by Nussinov et al., who examined allosteric mechanisms on cell signaling using molecular dynamics simulation (Nussinov et al., 2014).

Multidrug-resistant TB (MDR-TB) is concerned becomes a significant health issue and burden for TB patients particularly in Indonesia due to the frequency of increasing TB resistance is getting higher. MDR-TB does not respond at least to the isoniazid and rifampicin, the two most potent anti-TB drugs. Current treatment for drug-susceptible TB should contain the standard four-drug regimen consisting of isoniazid (H), rifampicin (R), ethambutol (E) and pyrazinamide (Z) for six months due to premature treatment interruption can cause drug resistance. Even it showed high efficacy; however, the regimen is not always well-tolerated in drug dosage and absorption. Moreover, the regimen often time gives side effects and severe adverse conditions, such as hepatotoxicity (Tiberi et al., 2018; Matteelli et al., 2018). Thus drug discovery and development of TB infection is a significant key for TB treatment and control. TB drug development had faced dormancy for decades.

Interestingly, recent efforts from many research groups have awakened a promising TB drug pipeline. Several new anti-TB agents, both synthetic and natural sources, are simultaneously studied in clinical trials by showing potential anti-TB activity in the hit to lead and lead optimization stages (Poce et al., 2014; Hoagland et al., 2016). There is

some database of constituents from medicinal plants available in open sources. These databases provide information on the three-dimensional structures of natural compounds of medicinal plants as bioactive in the multi-treatment diseases, including HIV-AIDS, TB, cancer, cardiovascular, inflammation, multiple sclerosis and many more (Yanuar et al., 2011; Afendi et al., 2011). In vitro studies had been reported that bioactive compounds from *Pluchea indica*, and *Rhoeo spathacea* plants in aqueous extracts showed good antimycobacterial activity against MDR strains and could be useful as a complementary alternative therapy against MDR-TB (Radji et al., 2015b).

There are skeptical thoughts that protein-based targeting cannot provide sufficient results to prevent lung disease, including tuberculosis. Several researchers are currently trying to work on transcriptomics-based drugs. However, although it is very promising, many technical hurdles obstruct the wide application in the clinics. Therefore, protein based-target is the most favorable and promising strategy, in particular for the treatment of TB diseases (Lechartier et al., 2014; Koli et al., 2014).

4. Conclusion

In this work, molecular docking and molecular dynamics simulation have been successfully employed to screen natural molecules isolated from *Rhoeo spathacea* and *Pluchea indica* and their derivatives as potential antimycobacterial compounds by inhibiting *M. tuberculosis* CYP121. Two ligands, i.e. kaempferol (KAE) and its benzyl derivative (KAE3) are identified as the best CYP121 inhibitors based on their binding affinities and adherence to the Lipinski's rule. Results of molecular dynamics simulation indicate that KAE and KAE3 possess a unique inhibitory mechanism against CYP121 that is different from GGJ (control ligand). The control ligand alters the overall dynamics of the receptor, which is indicated by changes in residue flexibility away from CYP121 binding site. Meanwhile, the dynamic changes caused by the binding of KAE and KAE3 are isolated around the binding site of CYP121. These ligands can be developed for further biological activities.

Declaration of Competing Interest

The authors declare no conflict of interest.

Acknowledgment

The authors would like to thank Dr. Bimo Ario Tejo, UCSI University, Malaysia, for a valuable suggestion regarding the manuscript content. Ultimately, the authors express great gratitude to the Scientific Committee of UAJ, SU, UY and UNAS for supporting the CADD project.

Appendix A. Supplementary data

Supplementary material related to this article can be found, in the online version, at doi:https://doi.org/10.1016/j.compbiolchem.2020.107205.

References

Afendi, F.M., Okada, T., Yamazaki, M., Hirai-Morita, A., Nakamura, Y., Nakamura, K., Ikeda, S., Takahashi, H., Altaf-Ul-Amin, M., Darusman, L.K., Saito, K., 2011. KNApSAcK family databases: integrated metabolite–plant species databases for multifaceted plant research. Plant Cell Physiol. 53 (2) pp.e1-e1.

Alexandrov, A.I., Mileni, M., Chien, E.Y., Hanson, M.A., Stevens, R.C., 2008. Microscale fluorescent thermal stability assay for membrane proteins. Structure 16 (3), 351–359.

Alonso, H., Bliznyuk, A., Gready, J., 2006. Combining docking and molecular dynamic simulations in drug design. Med. Res. Rev. 26 (5), 531–568.

xxx.

Barry, C.E., Boshoff, H.I., Via, L.E., 2006. Target selection to shorten the course of tuberculosis chemotherapy. In: Yew, W. (Ed.), Development of Antituberculosis Drugs. Nova Production, New York, pp. 29–52.

Bermawie, N., 2004. Inventory, documentation, and status of medicinal plants research in Indonesia. In: In: Batugal, P., Kaniyah, J., L. S.Y, Oliver, J. (Eds.), Medicinal Plant Research In Asia Volume 1. The Framework and *Project Workplans*. Serdang, Selangor: International Plant Genetic Resources Institute, pp. 104–112 [Accessed 10 November 2016].

CDC, 2015. Infectious Disease Related to Travel. [Online] Available at:. http://wwwnc.cdc.gov/travel/yellowbook/2016/infectious-diseasesrelated-to-travel/tuberculosis.

Chinsembu, K.C., 2016. Tuberculosis and nature's pharmacy of putative anti-tuberculosis agents. Acta Trop. 153, 46–56 28-31.

Collins, D., Hafidz, F., Suraratdecha, C., 2013. The Economic Burden of Tuberculosis in Indonesia. TB CARE I - Management Sciences for Health., Cambridge.

Hanwell, M.D., et al., 2012. Avogadro: an advanced semantic chemical editor, visualization, and analysis platform. J. Cheminform. 4, 17.

Hoagland, D.T., Liu, J., Lee, R.B., Lee, R.E., 2016. New agents for the treatment of drug-resistant Mycobacterium tuberculosis. Adv. Drug Deliv. Rev. 102, 55–72.

Jayaram, B., et al., 2012a. Sanjeevini: a freely accessible web-server for target directed lead molecule discovery. BMC Bioinformatics 13 (Suppl 17), S7.

Jayaram, B., Singh, T., Mukherjee, G., Mathur, A., Shekhar, S., Shekhar, V., 2012b. December. Sanjeevini: a Freely Accessible Web-Server for Target Directed Lead Molecule Discovery. In BMC Bioinformatics Vol. 13 BioMed Central No. 17, p. S7.

Kanabus, A., 2016. Information about Tuberculosis. [Online] Available at: http://www.tbfacts.org/tb/ [Accessed 28 June 2016]. .

Kim, S., et al., 2016. PubChem: STanubstance and compound databases. Nucleic Acids Res. 44, 1202–1213.

Koli, U., Krishnan, R.A., Pofali, P., Jain, R., Dandekar, P., 2014. SiRNA-based therapies for pulmonary diseases. J. Biomed. Nanotechnol. 10 (9), 1953–1997.

Krieger, E., Koraimann, G., Vriend, G., 2002. Increasing the precision of comparative models with YASARA NOVA—a self-parameterizing force field. Proteins 47 (3), 393–402.

Laskowski, R., Swindells, M., 2011. LigPlot+: multiple ligand-protein interaction diagrams for drug discovery. J. Chem. Inf. Model. 51, 2778–2786.

Lechartier, B., Rybniker, J., Zumla, A., Cole, S.T., 2014. Tuberculosis drug discovery in the post-post-genomic era. EMBO Mol. Med. 6 (2), 158–168.

Leys, D., et al., 2002. Atomic structure of *Mycobacterium tuberculosis* CYP121 to 1.06 Å reveals novel features of cytochrome P450. J. Biol. Chem. 278, 5141–5147.

Lipinski, C.A., Lombardo, F., Dominy, B.W., Feeney, P.J., 1997. Experimental and computational approach to estimate solubility and permeability in drug discovery and development settings. Adv. Drug Deliv. Rev. 23, 3–25.

Matteelli, A., Rendon, A., Tiberi, S., Al-Abri, S., Voniatis, C., Carvalho, A.C.C., Centis, R., D'Ambrosio, L., Visca, D., Spanevello, A., Migliori, G.B., 2018. Tuberculosis elimination: where are we now? Eur. Respir. Rev. 27 (148), 180035.

McLean, K.J., et al., 2008. Characterization of active site structure in Cyp121-A cytochrome P450 essential for viability of *Mycobacterium tuberculosis* H37rv. J. Biol. Chem. 283 (3), 33406–33416.

Miller, R.L., Thompson, A.A., Trapella, C., et al., 2015. The importance of ligand receptor conformational pairs in stabilization: spotlight on the N/OFQ G protein coupled receptor. Structure (London, England : 1993) 23 (12), 2291–2299.

Ministry of Health RI, 2011. Strategi Nasional Pengendalian TB di Indonesia 2010-2014. STOP TB.

Mohamad, S., Zin, N.M., Wahab, H.A., Ibrahim, P., Sulaiman, S.F., Zahariluddin, A.S., Noor, S.S., 2011. Antituberculosis potential of some ethnobotanically selected Malaysian plants. J. Ethnopharmacol. 133 (3), 1021–1026.

Nussinov, R., Tsai, C., Liu, J., 2014. Principles of allosteric interactions in cell signaling. J. Am. Chem. Soc. 136 (51), 17692–17701.

Nzila, A., Ma, Z., Chibale, K., 2011. Drug repositioning in the treatment of malaria and TB. Future Med. Chem. 3 (11), 1413–1426.

O'Boyle, N.M., et al., 2011. Open babel: an open chemical toolbox. J. Cheminform. 3, 33.

Oelschlaeger, P., Schmid, R., Pleiss, J., 2003. Modeling domino effects in enzymes: molecular basis of the substrate specificity of the bacterial metallo-betalactamases IMP-1 and IMP-6. Biochemistry 42 (30), 8945–8956.

Poce, G., Cocozza, M., Consalvi, S., Biava, M., 2014. SAR analysis of new anti-TB drugs currently in pre-clinical and clinical development. Eur. J. Med. Chem. 86, 335–351.

Radji, M., Kurniati, M., Kiranasari, A., 2015a. Comparative antimycobacterial activity of some Indonesian medicinal plants against multi-drug resistant *Mycobacterium tuberculosis*. J. Appl. Pharm. Sci. 5 (1), 019–022.

Radji, M., Kurniati, M., Kiranasari, A., 2015b. Comparative antimycobacterial activity of some Indonesian medicinal plants against multi-drug resistant Mycobacterium tuberculosis. J. Appl. Pharm. Sci. 5 (1), 019–022.

Ramyanti, N., Ariantari, N., Dwija, I., 2013. Aktivitas antituberkulosis kombinasi ekstrak N-heksana daun kedondong hutan dengan rifampisin terhadap isolat *Mycobacterium tuberculosis* strain MDR. J. Farm. Udayana 2 (3), 28–31.

Saleem, A., Azher, M., 2013. The next pandemic- tuberculosis: the oldest disease of mankind rising one more time. Br. J. Med. Practitioners 77 (6), 1205–1217.

Saludes, J.P., Garson, M.J., Franzblau, S.G., Aguinaldo, A.M., 2002. Antitubercular constituents from the hexane fraction of *Morinda citrifolia* Linn.(Rubiceae). Phytother. Res. 16, 683–685.

Skjaerven, L., Reuter, N., Martinez, A., 2011. Dynamics, flexibility and ligand-induced conformational changes in biological macromolecules: a computational approach. Future Med. Chem. 16, 2079–2100.

Sliwoski, G., Kothiwale, S., Meiler, J., Lowe, E.W., 2014. Computational methods in drug discovery. Pharmacol. Rev. 66 (1), 334–395.

Suriyaphan, O., 2014. Nutrition, health benefits and applications of *Pluchea indica* (L.) less leaves. J. Pharm. Sci. 41 (4), 1–10.

Tan, J.B.L., Lim, Y.Y., Lee, S.M., 2015. Antioxidant and antibacterial activity of *Rhoeo spathacea* (Swartz) Stearn leaves. J. Food Sci. Technol. 52 (4), 2394–2400.

Tiberi, S., Muñoz-Torrico, M., Duarte, R., Dalcolmo, M., D'Ambrosio, L., Migliori, G.B., 2018. New drugs and perspectives for new anti-tuberculosis regimens. Pulmonology 24 (2), 86–98.
Trott, O., Olson, A.J., 2010. AutoDock Vina: improving the speed and accuracy of docking with a new scoring function, efficient optimization and multithreading. J. Comput. Chem. 31, 455–461.
Vettoretti, G., et al., 2016. Molecular dynamics simulation reveal the mechanisms of allosteric activation of Hsp90 by designed ligands. Sci. Rep. 23830, 1–6.
Wallace, A., Laskowski, R., Thornton, J., 1996. LIGPLOT: a program to generate schematic diagrams of protein-ligand interactions. Protein Eng. 8, 127–134.
WHO, 2015. Global Tuberculosis Report 2015. 20th ed. WHO, Geneva.
Yanuar, A., Mun'im, A., Lagho, A.B.A., Syahdi, R.R., Rahmat, M., Suhartanto, H., 2011. Medicinal plants database and three dimensional structure of the chemical compounds from medicinal plants in Indonesia. arXiv preprint arXiv 1111, 7183.
Zhang, X., Stevens, R.C., Xu, F., 2015. The importance of ligands for G protein-coupled receptor stability. Trends Biochem. Sci. 40 (2), 79–87.
Zoete, V., Cuendet, M.A., Grosdidier, A., Michielin, O., 2011. SwissParam: a fast force field generation tool for small organic molecules. J. Comput. Chem. 32 (11), 2359–2368.

Structure-based discovery of novel inhibitors of Mycobacterium tuberculosis CYP121 from Indonesian natural products

ORIGINALITY REPORT

94%	12%	94%	4%
SIMILARITY INDEX	INTERNET SOURCES	PUBLICATIONS	STUDENT PAPERS

PRIMARY SOURCES

1	Vivitri Dewi Prasasty, Sandra Cindana, Fransiskus Xaverius Ivan, Hilyatuz Zahroh, Ernawati Sinaga. "Structure-based discovery of novel inhibitors of Mycobacterium tuberculosis CYP121 from Indonesian natural products", Computational Biology and Chemistry, 2020 Publication	93%
2	repository.ubaya.ac.id Internet Source	1%
3	suche.thulb.uni-jena.de Internet Source	<1%
4	Leitao, C.. "Fate of polyphenols and antioxidant activity of barley throughout malting and brewing", Journal of Cereal Science, 201205 Publication	<1%

Exclude quotes	On	Exclude matches	Off
Exclude bibliography	On		